

COMPARATIVE ANALYSIS ON MATHEMATICAL MODELS DESCRIBING VIBRATIONS OF AUTOMOTIVE INDEPENDENT SUSPENSIONS

Lilo Kunchev¹, Nikolay Pavlov

UDC: 519.87:629.012

INTRODUCTION

Kinematical structure of the vehicle independent suspension with increased speeds of motion have been refined over time and today there are a large number of its variants - single, double, and more arm suspensions. Underlying all these are single arm suspensions [6].

The aim of this work is using the methods of vector mechanics to analyze the results for both types of suspensions for the generalization of the computing process, which form the basis of an automated computer program to select the elastic characteristics of the suspension. Numerical experiments are conducted with MATLAB.

THREE-DIMENSIONAL MATHEMATICAL MODELS OF ARM SUSPENSIONS DESCRIBING THE SMOOTHNESS OF MOTION WITH THE METHODS OF VECTOR MECHANICS

The most accurate description behavior of the vehicle is achieved by using three-dimensional mathematical models. The advantage of such schemes is that it is possible to investigate the relocation of the car and turns along the axes O_x , O_y and O_z of the coordinate system located in the center of gravity (i.e. all degrees of freedom) which is a premise for high accuracy in computation process [7]. Schemes of the models are shown in Figure 1 and Figure 2.

The systems under consideration consists suspended and nosuspended masses. The suspended masses include the masses of the elements of the car body, passengers and load. In the center of gravity is fixed local coordinate system $O_0x_0y_0z_0$. The suspension is implemented as a tire, arm, axle and other components are combined in one element which is hinged to the suspended masses [10].

Each of these elements is fixed to local coordinate system, respectively $O_1x_1y_1z_1$, $O_2x_2y_2z_2$, $O_3x_3y_3z_3$, $O_4x_4y_4z_4$. In the equilibrium position the axis of the all coordinate systems are parallel. All displacements of local coordinate systems are given to the absolute coordinate system $O_Ax_Ay_Az_A$. For systems of Fig. 1 and Fig. 2 make the following assumptions [11]:

- elements of the system are solids;

¹Corresponding author e-mail: lkunchev@tu-sofia.bg, Technical University, Sofia

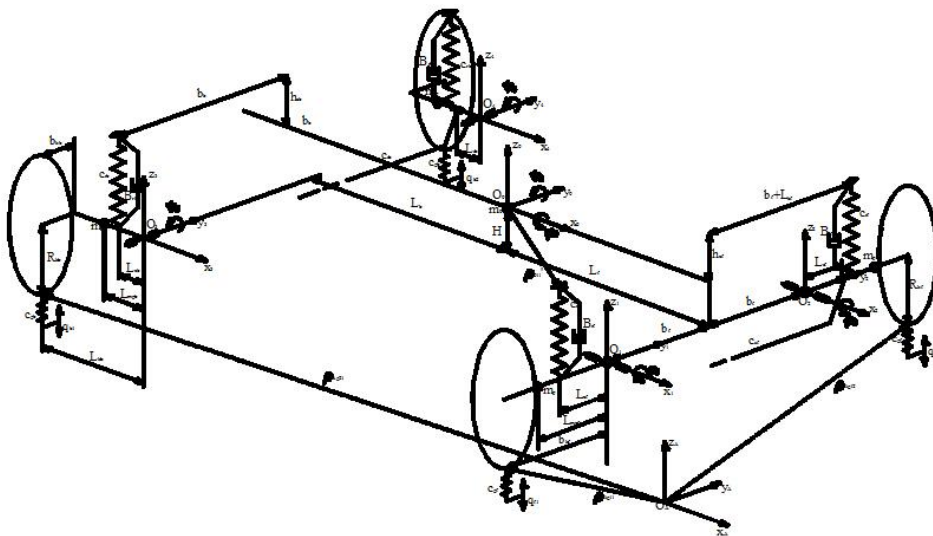


Figure 1: Kinematic scheme of a car with front transverse and rear longitudinal arms

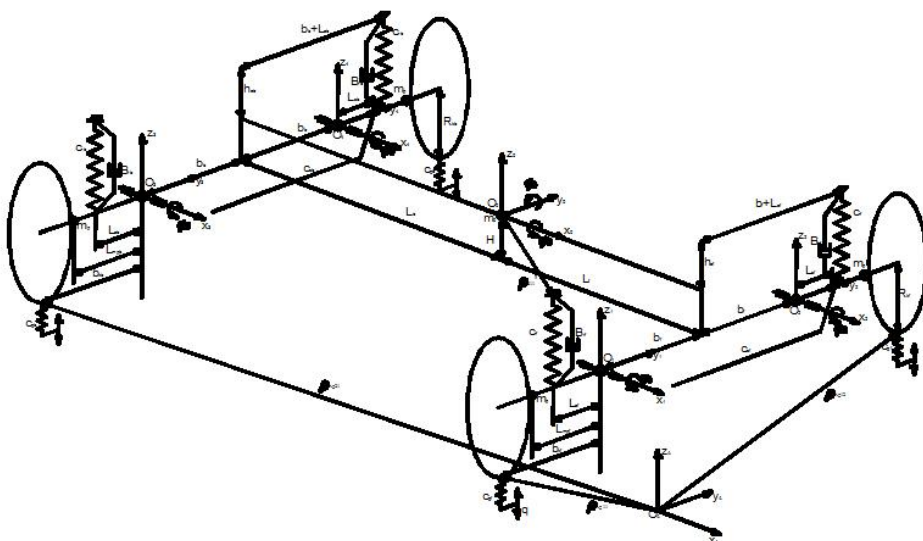


Figure 2: Kinematic scheme of a car with front and rear transverse arms

- anti-roll bars are massless and their stiffness is regarded as equivalent spring connected to the arms at point to a distance L_{sf} of the joint (hinge) of the front axle and L_{sb} of the joint of the rear axle;
- give an account damping and elastic properties of the main elements c_{rf} , c_{rb} , β_{rf} , β_{rb} , respectively, springs and shock absorbers the front and the rear axle, and the elasticity of the tire c_{gf} and c_{gb} the front and the rear axle;
- elastic and damping elements have linear characteristics;

- system is placed in a equilibrium position as the centers of gravity to the wheels lie on a horizontal axis. O_1y_1 axis coincides with the axis O_2y_2 , and O_3y_3 axis coincides with O_4y_4 .

For generalized coordinate systems are adopted:

- z_0 - linear displacement of the local coordinate system $O_0x_0y_0z_0$ to absolute $O_{Ax}A_yA_zA$ on axis O_z ;
- φ_0, ψ_0 - angular displacement of the local coordinate system $O_0x_0y_0z_0$ to absolute $O_{Ax}A_yA_zA$ respectively around the axes O_x and O_y ;
- φ_1 - angular displacement around the axis O_1x_1 of the coordinate system $O_1x_1y_1z_1$;
- φ_2 - angular displacement around the axis O_2x_2 of the coordinate system $O_2x_2y_2z_2$;
- φ_3 - angular displacement around the axis O_3x_3 of the coordinate system $O_3x_3y_3z_3$;
- φ_4 - angular displacement around the axis O_4x_4 of the coordinate system $O_4x_4y_4z_4$;
- ψ_3 - angular displacement around the axis O_3y_3 of the coordinate system $O_3x_3y_3z_3$;
- ψ_4 - angular displacement around the axis O_4y_4 of the coordinate system $O_4x_4y_4z_4$;

To find laws of motion in the absolute coordinate system $O_{Ax}A_yA_zA$ is necessary to define the transition matrices of each local coordinate systems to the absolute.

Matrix of transition from $O_0x_0y_0z_0$ to $O_{Ax}A_yA_zA$ for Fig. 1 and 2 is:

$$T_0^A = \begin{bmatrix} \cos \psi_0 & 0 & -\sin \psi_0 & 0 \\ -\sin \varphi_0 \cdot \sin \psi_0 & \cos \varphi_0 & -\sin \varphi_0 \cdot \cos \psi_0 & 0 \\ \cos \varphi_0 \cdot \sin \psi_0 & \sin \varphi_0 & \cos \varphi_0 \cdot \cos \psi_0 & z_0 \\ 0 & 0 & 0 & 1 \end{bmatrix} \quad (1)$$

x_0 and y_0 are zero because is consider only linear oscillation on axis Oz , i.e. only vertically; Matrix of transition from $O_1x_1y_1z_1, O_2x_2y_2z_2, O_3x_3y_3z_3, O_4x_4y_4z_4$, to $O_0x_0y_0z_0$ have a type:

For Figure 1:

$$T_1^0 = \begin{bmatrix} 1 & 0 & 0 & L_f \\ 0 & \cos \varphi_1 & -\sin \varphi_1 & -b_f \\ 0 & \sin \varphi_1 & \cos \varphi_1 & -H \\ 0 & 0 & 0 & 1 \end{bmatrix} \quad T_3^0 = \begin{bmatrix} \cos \psi_3 & 0 & -\sin \psi_3 & -L_b \\ 0 & 1 & 0 & -b_b \\ \sin \psi_3 & 0 & \cos \psi_3 & -H \\ 0 & 0 & 0 & 1 \end{bmatrix} \quad (2)$$

$$T_2^0 = \begin{bmatrix} 1 & 0 & 0 & L_f \\ 0 & \cos \varphi_2 & -\sin \varphi_2 & b_f \\ 0 & \sin \varphi_2 & \cos \varphi_2 & -H \\ 0 & 0 & 0 & 1 \end{bmatrix} \quad T_4^0 = \begin{bmatrix} \cos \psi_4 & 0 & -\sin \psi_4 & -L_b \\ 0 & 1 & 0 & b_b \\ \sin \psi_4 & 0 & \cos \psi_4 & -H \\ 0 & 0 & 0 & 1 \end{bmatrix}$$

For Figure 2 only T_3^0 and T_4^0 are different:

$$T_3^0 = \begin{bmatrix} 1 & 0 & 0 & -L_b \\ 0 & \cos \varphi_3 & -\sin \varphi_3 & -b_b \\ 0 & \sin \varphi_3 & \cos \varphi_3 & -H \\ 0 & 0 & 0 & 1 \end{bmatrix} \quad T_4^0 = \begin{bmatrix} 1 & 0 & 0 & -L_b \\ 0 & \cos \varphi_4 & -\sin \varphi_4 & b_b \\ 0 & \sin \varphi_4 & \cos \varphi_4 & -H \\ 0 & 0 & 0 & 1 \end{bmatrix} \quad (3)$$

After multiplying the matrices and simplify the resulting expressions for the components of the angular velocity of arms to three axes:

For Figure 1:

-front right arm:

$$\begin{aligned} \omega_{1x}^A &= \dot{\varphi}_0 + \dot{\varphi}_1 \cos \psi_0 & \omega_{1y}^A &= \dot{\psi}_0 \cos \varphi_0 + \dot{\varphi}_1 \sin \psi_0 \sin \varphi_0 \\ \omega_{1z}^A &= \dot{\varphi}_1 \sin \psi_0 \cos \varphi_0 - \dot{\psi}_0 \sin \varphi_0 \end{aligned} \quad (4)$$

After removal of terms of a higher order is received:

$$\omega_{1x}^A = \dot{\varphi}_0 + \dot{\varphi}_1 \quad \omega_{1y}^A = \dot{\psi}_0 \quad \omega_{1z}^A = 0 \quad (5)$$

Similarly to determine the angular velocities of the other arms:

-front left arm:

$$\omega_{2x}^A = \dot{\varphi}_0 + \dot{\varphi}_2 \quad \omega_{2y}^A = \dot{\psi}_0 \quad \omega_{2z}^A = 0 \quad (6)$$

- rear right arm:

$$\omega_{3x}^A = \dot{\varphi}_0 \quad \omega_{3y}^A = \dot{\psi}_0 + \dot{\psi}_3 \quad \omega_{3z}^A = 0 \quad (7)$$

- rear left arm:

$$\omega_{4x}^A = \dot{\varphi}_0 \quad \omega_{4y}^A = \dot{\psi}_0 + \dot{\psi}_4 \quad \omega_{4z}^A = 0 \quad (8)$$

For Figure 2 is only different angular speeds of the rear arms:

- rear right arm:

$$\omega_{3x}^A = \dot{\phi}_0 + \dot{\phi}_3 \quad \omega_{3y}^A = \dot{\psi}_0 \quad \omega_{3z}^A = 0 \quad (9)$$

- rear left arm:

$$\omega_{4x}^A = \dot{\phi}_0 + \dot{\phi}_4 \quad \omega_{4y}^A = \dot{\psi}_0 \quad \omega_{4z}^A = 0 \quad (10)$$

Kinetic energies of two systems are:

For Figure 1:

$$\begin{aligned} T = & \frac{1}{2} m_0 \dot{z}_0^2 + \frac{1}{2} J_{0x} \dot{\phi}_0^2 + \frac{1}{2} J_{0y} \dot{\psi}_0^2 + \frac{1}{2} J_{pxf} (\dot{\phi}_0 + \dot{\phi}_1)^2 + \frac{1}{2} J_{pxf} (\dot{\phi}_0 + \dot{\phi}_2)^2 + \\ & + \frac{1}{2} J_{pyb} (\dot{\psi}_0 + \dot{\psi}_3)^2 + \frac{1}{2} J_{pyb} (\dot{\psi}_0 + \dot{\psi}_4)^2 + \\ & + 2\left(\frac{1}{2} J_{pyf} \dot{\psi}_0^2\right) + 2\left(\frac{1}{2} J_{pxb} \dot{\phi}_0^2\right) + \frac{1}{2} m_p (\dot{z}_0 - (L_{mpf} + b_f) \dot{\phi}_0 + L_f \dot{\psi}_0 - L_{mpf} \dot{\phi}_1)^2 + \\ & + \frac{1}{2} m_p (\dot{z}_0 + (L_{mpf} + b_f) \dot{\phi}_0 + L_f \dot{\psi}_0 + L_{mpf} \dot{\phi}_2)^2 + \\ & + \frac{1}{2} m_p (\dot{z}_0 - b_b \dot{\phi}_0 - (L_{mpb} + L_b) \dot{\psi}_0 - L_{mpb} \dot{\psi}_3)^2 + \\ & + \frac{1}{2} m_p (\dot{z}_0 + b_b \dot{\phi}_0 - (L_{mpb} + L_b) \dot{\psi}_0 - L_{mpb} \dot{\psi}_4)^2 \end{aligned} \quad (11)$$

For Figure 2:

$$\begin{aligned} T = & \frac{1}{2} m_0 \dot{z}_0^2 + \frac{1}{2} J_{0x} \dot{\phi}_0^2 + \frac{1}{2} J_{0y} \dot{\psi}_0^2 + \frac{1}{2} J_{pxf} (\dot{\phi}_0 + \dot{\phi}_1)^2 + \\ & + \frac{1}{2} J_{pxf} (\dot{\phi}_0 + \dot{\phi}_2)^2 + \frac{1}{2} J_{pxb} (\dot{\phi}_0 + \dot{\phi}_3)^2 + \frac{1}{2} J_{pxb} (\dot{\phi}_0 + \dot{\phi}_4)^2 + \\ & + 2\left(\frac{1}{2} J_{pyf} \dot{\psi}_0^2\right) + 2\left(\frac{1}{2} J_{pyb} \dot{\psi}_0^2\right) + \frac{1}{2} m_p (\dot{z}_0 - (L_{mpf} + b_f) \dot{\phi}_0 + L_f \dot{\psi}_0 - L_{mpf} \dot{\phi}_1)^2 + \\ & + \frac{1}{2} m_p (\dot{z}_0 + (L_{mpf} + b_f) \dot{\phi}_0 + L_f \dot{\psi}_0 + L_{mpf} \dot{\phi}_2)^2 + \\ & + \frac{1}{2} m_p (\dot{z}_0 - (L_{mpb} + b_b) \dot{\phi}_0 - L_b \dot{\psi}_0 - L_{mpb} \dot{\psi}_3)^2 + \\ & + \frac{1}{2} m_p (\dot{z}_0 + (L_{mpb} + b_b) \dot{\phi}_0 - L_b \dot{\psi}_0 + L_{mpb} \dot{\psi}_4)^2 \end{aligned} \quad (12)$$

Potential energies of the two systems are:

For Figure 1:

$$\begin{aligned}
\Pi = & \frac{1}{2}c_{rf}(L_{cf}\varphi_1)^2 + \frac{1}{2}c_{rf}(-L_{cf}\varphi_2)^2 + \frac{1}{2}c_{rb}(L_{cb}\psi_3)^2 + \frac{1}{2}c_{rb}(L_{cb}\psi_4)^2 + \\
& + \frac{1}{2}c_{gz}(z_0 - (b_f + b_{kf})\varphi_0 + L_f\psi_0 - b_{kf}\varphi_1 - q_{f1})^2 + \\
& + \frac{1}{2}c_{gz}(z_0 + (b_f + b_{kf})\varphi_0 + L_f\psi_0 + b_{kf}\varphi_2 - q_{f2})^2 + \\
& + \frac{1}{2}c_{gz}(z_0 - (b_b + b_{kb})\varphi_0 - (L_b + L_{kb})\psi_0 - L_{kb}\psi_3 - q_{b1})^2 + \\
& + \frac{1}{2}c_{gz}(z_0 + (b_b + b_{kb})\varphi_0 - (L_b + L_{kb})\psi_0 - L_{kb}\psi_4 - q_{b2})^2 \\
& + \frac{1}{2}c_{sf}(-L_{sf}\varphi_1 - L_{sf}\varphi_2)^2 + \frac{1}{2}c_{sb}(-L_{sb}\psi_3 + L_{sb}\psi_4)^2
\end{aligned} \tag{13}$$

For Figure 2:

$$\begin{aligned}
\Pi = & \frac{1}{2}c_{rf}(L_{cf}\varphi_1)^2 + \frac{1}{2}c_{rf}(-L_{cf}\varphi_2)^2 + \frac{1}{2}c_{rb}(L_{cb}\varphi_3)^2 + \\
& + \frac{1}{2}c_{rb}(-L_{cb}\varphi_4)^2 + \frac{1}{2}c_{gz}(z_0 - (b_f + b_{kf})\varphi_0 + L_f\psi_0 - b_{kf}\varphi_1 - q_{f1})^2 + \\
& + \frac{1}{2}c_{gz}(z_0 + (b_f + b_{kf})\varphi_0 + L_f\psi_0 + b_{kf}\varphi_2 - q_{f2})^2 + \\
& + \frac{1}{2}c_{gz}(z_0 - (b_b + b_{kb})\varphi_0 - L_b\psi_0 - b_{kb}\varphi_3 - q_{b1})^2 + \\
& + \frac{1}{2}c_{gz}(z_0 + (b_b + b_{kb})\varphi_0 - L_b\psi_0 + b_{kb}\varphi_4 - q_{b2})^2 \\
& + \frac{1}{2}c_{sf}(-L_{sf}\varphi_1 - L_{sf}\varphi_2)^2 + \frac{1}{2}c_{sb}(-L_{sb}\varphi_3 - L_{sb}\varphi_4)^2
\end{aligned} \tag{14}$$

The Rayleigh's functions are:

For Figure 1:

$$R = \frac{1}{2}\beta_{rf}(L_{cf}\dot{\varphi}_1)^2 + \frac{1}{2}\beta_{rf}(-L_{cf}\dot{\varphi}_2)^2 + \frac{1}{2}\beta_{rb}(L_{cb}\dot{\psi}_3)^2 + \frac{1}{2}\beta_{rb}(L_{cb}\dot{\psi}_4)^2 \tag{15}$$

For Figure 2:

$$R = \frac{1}{2}\beta_{rf}(L_{cf}\dot{\varphi}_1)^2 + \frac{1}{2}\beta_{rf}(-L_{cf}\dot{\varphi}_2)^2 + \frac{1}{2}\beta_{rb}(L_{cb}\dot{\varphi}_3)^2 + \frac{1}{2}\beta_{rb}(-L_{cb}\dot{\varphi}_4)^2 \tag{16}$$

After applying Lagrange's equation of 2nd kind:

$$\frac{d}{dt}\left(\frac{\partial T}{\partial \dot{q}}\right) - \left(\frac{\partial T}{\partial q}\right) = -\left(\frac{\partial \Pi}{\partial q}\right) - \left(\frac{\partial R}{\partial \dot{q}}\right) \tag{17}$$

For equations describing the laws of motion of the system is valid:

$$[M]\ddot{q} + [B]\dot{q} + [C]q = [F] \tag{18}$$

- [M] is the matrix of inertia that is symmetrical with the main diagonal with dimension 7x7 and she has the following form:

$m_p + 4m_p$	0	$2m_p L_r$	$-m_p L_{maf}$	$m_p L_{maf}$	$-m_p L_{mab}$	$-m_p L_{mab}$
$-m_p L_{mab}$	$J_{ox} + 2J_{oxf} + 2J_{oxb} + 2m_p b_b^2 + 2m_p (L_{maf} + b_f)^2$	0	$J_{oxf} + m_p L_{maf}$	$J_{oxf} + m_p L_{maf}$	$m_p b_b L_{mab}$	$-m_p b_b L_{mab}$
$2m_p L_r - 2m_p (L_{mab} + L_b)$	$J_{ox} + 2J_{oxf} + 2J_{oxb} + 2m_p b_b^2 + 2m_p (L_{maf} + b_f)^2$	0	$J_{oxf} + m_p L_{maf}$	$J_{oxf} + m_p L_{maf}$	$J_{oxb} + m_p L_{mab}$	$J_{oxb} + m_p L_{mab}$
$2m_p L_r - 2m_p L_b$	$J_{oy} + 2J_{oyf} + 2J_{oyb} + 2m_p L_r^2 + 2m_p (L_{mab} + L_b)^2$	$J_{oy} + 2J_{oyf} + 2J_{oyb} + 2m_p L_r^2 + 2m_p (L_{mab} + L_b)^2$	$-m_p L_{maf}$	$m_p L_{maf}$	$m_p L_b L_{mab}$	$-m_p L_b L_{mab}$
$-m_p L_{maf}$	$J_{oxf} + m_p L_{maf}$	$-m_p L_{maf}$	$J_{oxf} + m_p L_{maf}^2$	0	0	0
$m_p L_{maf}$	$J_{oxf} + m_p L_{maf}$	$m_p L_{maf}$	0	$J_{oxf} + m_p L_{maf}^2$	0	0
$-m_p L_{mab}$	$m_p b_b L_{mab}$	$J_{oyb} + m_p L_{mab}$	0	0	$J_{oyb} + m_p L_{mab}^2$	0
$-m_p L_{mab}$	$-m_p b_b L_{mab}$	$-m_p b_b L_{mab}$	0	0	0	$J_{oyb} + m_p L_{mab}^2$
$m_p L_{mab}$	$J_{oxb} + m_p L_{mab}$	$-m_p L_b L_{mab}$	0	0	0	$J_{oxb} + m_p L_{mab}^2$

- [C] is the matrix of elasticity, which is also symmetric and has dimension 7x7

$4C_{gz}$	0	$2C_{gz}L_f - 2C_{gz} \frac{(L_g + L_{kb})}{L_g + L_{kb}}$	$-C_{gz}b_{kf}$	$C_{gz}b_{kf}$	$-C_{gz}L_{kb}$	$-C_{gz}L_{kb}$
0	$2C_{gz}(b_f + b_{kf})^2 + 2C_{gz}(b_b + b_{kb})^2$	0	$C_{gz}b_{kf}(b_f + b_{kf})$	$C_{gz}b_{kf}(b_f + b_{kf})$	$C_{gz}L_{kb}(b_b + b_{kb})$	$C_{gz}b_{kb}(b_b + b_{kb})$
$2C_{gz}L_f - 2C_{gz} \frac{(L_g + L_{kb})}{L_g + L_{kb}}$	0	$2C_{gz}L_f^2 + 2C_{gz} \frac{(L_b + L_{kb})^2}{(L_b + L_{kb})^2}$	$-C_{gz}b_{kf}L_f$	$C_{gz}b_{kf}L_f$	$C_{gz}L_{kb}$	$C_{gz}L_{kb} \frac{(L_b + L_{kb})}{(L_b + L_{kb})}$
$-C_{gz}b_{kf}$	$C_{gz}b_{kf}(b_f + b_{kf})$	$-C_{gz}b_{kf}L_f$	$C_{kf}L_{kf}^2 + C_{gz}b_{kf}^2 + C_{sf}L_{sf}^2$	$C_{sf}L_{sf}^2$	0	0
$C_{gz}b_{kf}$	$C_{gz}b_{kf}(b_f + b_{kf})$	$C_{gz}b_{kf}L_f$	$C_{sf}L_{sf}^2$	$C_{kf}L_{kf}^2 + C_{gz}b_{kf}^2 + C_{sf}L_{sf}^2$	0	0
$-C_{gz}L_{kb}$	$C_{gz}L_{kb}(b_b + b_{kb})$	$C_{gz}L_{kb}(L_b + L_{kb})$	0	0	$C_{fb}L_{fb}^2 + C_{gz}L_{kb}^2 + L_{kb}^2 + C_{sb}L_{sb}^2$	$-C_{sb}L_{sb}^2$
$C_{gz}b_{kb}$	$C_{gz}b_{kb}(b_b + b_{kb})$	$C_{gz}b_{kb}L_b$	0	0	$C_{fb}L_{fb}^2 + C_{gz}b_{kb}^2 + C_{sb}L_{sb}^2$	$C_{sb}L_{sb}^2$
$-C_{gz}L_{kb}$	$-C_{gz}L_{kb}(b_b + b_{kb})$	$C_{gz}L_{kb}(L_b + L_{kb})$	0	0	$-C_{sb}L_{sb}^2$	$C_{fb}L_{fb}^2 + C_{gz}L_{kb}^2 + C_{sb}L_{sb}^2$
$C_{gz}b_{kb}$	$C_{gz}b_{kb}(b_b + b_{kb})$	$-C_{gz}b_{kb}L_b$	0	0	$C_{fb}L_{fb}^2 + C_{gz}b_{kb}^2 + C_{sb}L_{sb}^2$	$C_{fb}L_{fb}^2 + C_{gz}b_{kb}^2 + C_{sb}L_{sb}^2$

Cells colored in Lt Dwn Diagonal refer to the system of Figure 1 and those in gray (light) of Figure 2.

- [B] is the matrix of dissipative forces, showing the influence of damper - symmetric with dimension 7x7:

0	0	0	0	0	0	0
0	0	0	0	0	0	0
0	0	0	0	0	0	0
0	0	0	$\beta_{rf} \cdot L_{cf}^2$	0	0	0
0	0	0	0	$\beta_{rf} \cdot L_{cf}^2$	0	0
0	0	0	0	0	$\beta_{rb} \cdot L_{cb}^2$	0
0	0	0	0	0	0	$\beta_{rb} \cdot L_{cb}^2$

To obtain natural frequencies of its system equations are presented in Cauchy normal form:

$$y + Ly = 0 \tag{19}$$

Where L is:

$$L = \begin{bmatrix} M^{-1}B & M^{-1}C \\ I & O \end{bmatrix} \tag{20}$$

The output parameters of the system are vibration displacement, vibration velocity, vibration acceleration and they are obtained from the equations:

$$y + Ly = Y \tag{21}$$

Where Y is:

$$Y = \begin{bmatrix} M^{-1}F(t) \\ O \end{bmatrix} \tag{22}$$

After integration of the system using the method of Runge - Kutta receive all decisions in a given time interval.

NUMERICAL INVESTIGATIONS

The main parameters and their numerical values are shown in table 1:

Table 1:

№	Parameter	Symbol	Value
1.	Suspended masses	m_0	1400 kg
2.	Nosuspended masses	m_p	30 kg
3.	Moment of inertia of the sprung masses around longitudinal axis (x-axis)	J_{0x}	550 kg.m ²
4.	Moment of inertia of the sprung masses around transverse axis (y-axis)	J_{0y}	2000 kg.m ²
5.	Moment of inertia of the unsprung masses on the front axle around x-axis	J_{pxf}	5 kg.m ²
6.	Moment of inertia of the unsprung masses on the rear axle around x-axis	J_{pxb}	2 kg.m ²
7.	Moment of inertia of the unsprung masses on the front axle around y-axis	J_{pyf}	2 kg.m ²
8.	Moment of inertia of the unsprung masses on the rear axle around y-axis	J_{pyb}	5 kg.m ²
9.	Vertical co-ordinate of the center of gravity of the unsprung masses in relation to joint of the arms	H	0,4 m
10.	Horizontal co-ordinate of the center of gravity of the unsprung masses in relation to joint of the front arms	b_f	0,4 m
11.	Horizontal co-ordinate of the center of gravity of the unsprung masses in relation to joint of the rear arms	b_b	0,6 m
12.	Distance from the center of gravity to the front axle	L_f	1,1 m
13.	Distance from the center of gravity to the rear axle	L_b	1,5 m
14.	Length of the front arm	b_{kf}	0,42 m
15.	Length of the rear arm	L_{kb}	0,42 m
16.	Distance from the contact point of the rear wheel to joint of the arm	b_{kb}	0,2 m
17.	Distance from the center of gravity of the front(f) and the rear(b) arm to the respective joint	L_{mp}	0,4 m
18.	Distance from fixing point of the front(f) and the rear(b) main elastic element to the respective joint	L_c	0,3 m
19.	Distance from fixing point of the front(f) and the rear(b) anti-roll bar to the respective joint	L_s	0,28 m
20.	Radius of the front(f) and the rear(b) wheels	R_k	0,26 m
21.	Stiffness coefficient of the main elastic elements of the front axle	c_{rf}	25000 N/m

№	Parameter	Symbol	Value
22.	Stiffness coefficient of the main elastic elements of the rear axle	c_{rb}	25000 N/m
23.	Stiffness coefficient of the tyre	c_{gz}	125000 N/m
24.	Stiffness coefficient of the anti-roll bars of the front(f) and the rear(b) axle	c_s	20000 N/m
25.	Damping coefficient of the front(f) and the rear(b) shock absorbers	β_r	1900 N.s/m

The parameters are not measured by authors and are taken from literary sources cited below.

Natural frequencies of the systems:

0.8099 Hz (for Fig.1) / 0.9839 Hz (for Fig. 2) - frequency of linear oscillations of suspended masses on z-axis;

1.6722 Hz / 1.7286 Hz - frequency of angular oscillation of the sprung masses around x-axis;

1.1740 Hz / 0.8367 Hz - frequency of angular oscillation of the sprung masses around y-axis;

7.8614 and 7.8506 Hz / 7.8593 and 7.8832 Hz - angular frequency of the front arms;

8.3490 and 8.3100 Hz / 8.2327 and 8.3100 Hz - angular frequency of the rear arms;

Disturbing actions in the system are sinusoidal and are attached in the center of the contact patch of the tire with the road. They have the following form:

$$q = q_0(1 - \cos(vt)) \quad (23)$$

$q_0 = 0,02$ m - height of the amplitude of roughness;

v - circular frequency of the disturbing action:

$$v = \frac{2\pi.V}{S}, \text{ rad/s} \quad (24)$$

The frequency of the disturbing action expressed in hertz:

$$v = \frac{1}{2\pi} \frac{2\pi.V}{S}, \text{ Hz} \quad (25)$$

V - velocity of the car, m / s;

S - wavelength, m.

As the maximum accelerations are important, the investigated of the behavior of individual

elements of the system was conducted at a frequency effects similar to their natural frequencies. The results obtained for some of the accelerations are shown in figures below:

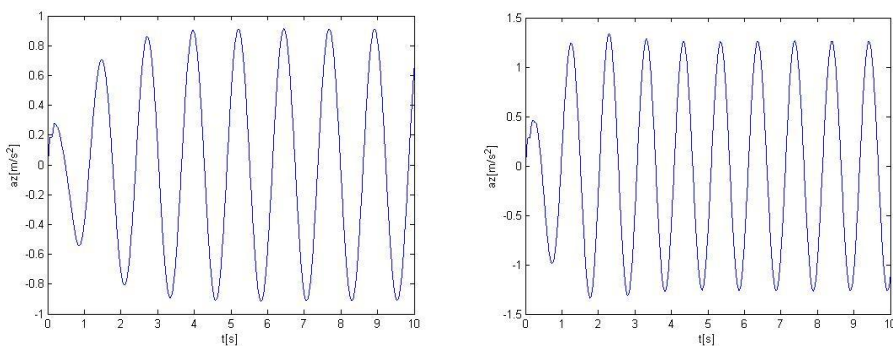


Figure 3: Linear acceleration of sprung masses on z-axis respectively of the models in Figure 1 and 2

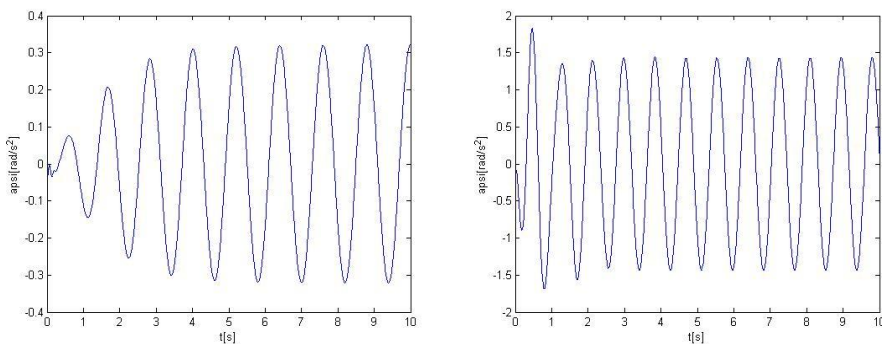


Figure 4: Angular acceleration of suspended masses on y-axis respectively of the models in Figure 1 and 2

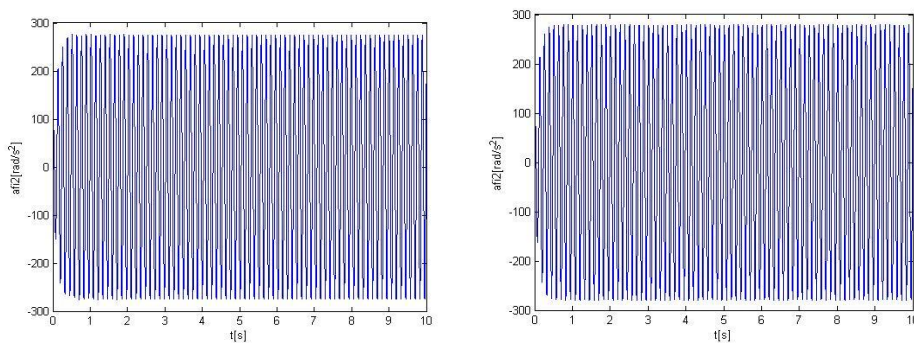


Figure 5: Angular acceleration of the front left arm of Figure 1 and 2

CONCLUSION

The generalization of the matrix of both automotive suspension may be used to create automated software to set its computing part and thus to accelerate the work in choosing the type of suspension and its elastic parameters.

ACKNOWLEDGEMENT

This work is a part of the research project to support of PhD students № 102ПД021-4 funded by Research Centre at Technical University – Sofia.

REFERENCES

- [1] Demic, M., Diligenski, D., Demic, I., Demic, M. A method of vehicle active suspension design. Springer – Verlag, 2006.
- [2] Ellis, J.R. Vehicle Dynamics. London Business Books Limited, 1975.
- [3] Genta, G. Motor Vehicle Dynamics. Word Scientific, 1997.
- [4] Hirshberg, W. Fahrzeugdynamic. 1997.
- [5] Katzov, D., D. Hlebarski. Kinematiks of the turn of wheel vehicle with account of the tires and influence of the suspension. International Journal of Pure and Applied Mathematics, Vol 25, № 2, 2005.
- [6] Kunchev, L.P., G.M. Yanachkov. Изследване динамичното поведение на раменно окачване.
- [7] Kunchev, L.P., G.M. Yanachkov. Моделиране плавността на движение на автомобил с еднораменно окачване. trans&MOTAUTO'05, Велико Търново, 2005.
- [8] Русев, Р., П. Партинов, Т. Тодоров. Свободни трептения на системата трансмисия – окачване. Петнадесети национален семинар „Динамика на механични системи”, Варна, 1990.
- [9] Яначков, Г.М. Изследване динамичното поведение на предно раменно окачване тип Макферсон, trans&MOTAUTO'06.
- [10] Kunchev, L.P., G.M. Yanachkov. Изследване динамичното поведение на автомобил с раменно окачване. trans&MOTAUTO'06.
- [11] Kunchev, L., G. Yanachkov. Comparison analyze on the theoretical mechanic mathematical models, describing arm suspensions. MVM, Kragujevac, 4th – 6th October 2006, Serbia.

